Long-wave infrared generation from femtosecond and picosecond optical parametric oscillators based on orientation-patterned gallium phosphide

Applied Physics B (2018) 124:143
https://doi.org/10.1007/s00340-018-7001-2

Applied Physics B
Lasers and Optics

Long-wave infrared generation from femtosecond and picosecond optical parametric oscillators based on orientation-patterned gallium phosphide

Luke Maidment[1,2] · Oguzhan Kara[1] · Peter G. Schunemann[3] · Jonathon Piper[4] · Kenneth McEwan[4] · Derryck T. Reid[1]

Received: 30 January 2018 / Accepted: 2 June 2018

Abstract
Optical parametric oscillators synchronously pumped with 1-μm femtosecond and picosecond lasers are used to generate long-wave mid-infrared radiation using the nonlinear material orientation-patterned gallium phosphide. The output spectra from the femtosecond OPO are measured, demonstrating tuning based on grating period and temperature from 5.5 to 13.0 μm. The picosecond OPO produces 137 mW at 7.87 μm, representing the first picosecond-pumped OPO using orientation gallium phosphide.

1 Introduction

Sources of coherent mid-infrared radiation have a range of applications including spectroscopy and high field physics. Mid-infrared (mid-IR) absorption spectroscopy benefits from spatial coherence as it allows long path lengths to be investigated [1], and allows tight focusing for microspectroscopy [2]. Quantum cascade lasers (QCLs), while a commercially available and mature laser technology, are generally narrow linewidth offering limited tuning, though external cavity QCLs (EC-QCLs) have been demonstrated with considerable, rapid tuning [3, 4], and there are also commercially available (EC-QCLs) containing several QCL chips, with wide tuning across the mid-IR (for example [5]). QCLs have become the source of choice for many applications requiring coherent mid-IR light, although nonlinear optical sources still offer some advantages in achieving high pulse energy or short pulse durations, and in achieving instantaneous coverage of a broad mid-IR wavelength range. Flexibility with repetition rates also means dual-comb spectroscopy (DCS) [6] has been explored much more widely with nonlinear mid-IR sources.

Reaching the long-wave mid-IR (8–14 μm) at high-repetition rates and with useful power levels has until recently proven very difficult. Oxide-based materials such as periodically poled lithium niobate (PPLN), periodically poled potassium titanyl phosphate (PPKTP) and periodically poled potassium titanyl arsenate (PPKTA) offer excellent performance below 5 μm and are routinely employed for parametric generation in this region. Multi-phonon absorption makes these materials opaque above ~5 μm due to multi-phonon absorption, and their nonlinear figure of merits [7]—functions of refractive index and of the effective second order nonlinearity d_{eff}—are poor compared to alternative semiconductor crystals which are now becoming more readily available.

This paper concentrates on the application of one such semiconductor nonlinear crystal, orientation-patterned gallium phosphide (OPGaP), as a mean of efficiently producing ps and fs pulses in the long-wave mid-IR above 7 μm. Its performance in terms of figure-of-merit and transmission is

This article is part of the topical collection "Mid-infrared and THz Laser Sources and Applications" guest edited by Wei Ren, Paolo De Natale and Gerard Wysocki.

✉ Luke Maidment
lm345@hw.ac.uk

[1] Scottish Universities Physics Alliance (SUPA), Institute of Photonics and Quantum Sciences, School of Engineering and Physical Sciences, Heriot-Watt University, Edinburgh EH14 4AS, UK

[2] Chromacity Ltd., Livingstone House, 43 Discovery Terrace, Research Avenue North, Riccarton, Edinburgh EH14 4AP, UK

[3] BAE Systems, Inc., MER15-1813, P.O. Box 868, Nashua, NH 03061-0868, USA

[4] Defence Science and Technology Laboratory, Porton Down, Salisbury SP4 0JQ, UK

Published online: 23 June 2018

compared in Fig. 1 with that of ten other contemporary nonlinear materials which can be used to generate mid-IR wavelengths. Regions where the materials do transmit but where parametric generation or pumping is problematic due to two-photon absorption or no phasematching condition are greyed out. Cadmium silicon phosphide ($CdSiP_2$ or CSP) has been used in OPOs to generate mid-IR from 6 to 8 µm, in a range of configurations using 1-µm ps and fs pump lasers, as well as using an optical parametric oscillator (OPO) as the pump (discussed in the recent review by Kumar et al. [8]). CSP has also been used recently in an optical parametric amplifier to generate short duration pulse spanning 4.4–9.0 µm [9]. Zinc germanium phosphide ($ZnGeP_2$ or ZGP) requires a pump laser with 1.9-µm wavelength or higher, meaning less mature laser sources must be used. It has been used to generate high energy pulses in an optical parametric amplifier between 6 and 7.5 µm [10].

Orientation-patterned gallium arsenide (OPGaAs) has good transmission up to 17 µm, but due to two-photon absorption requires a pump laser of 1.7 µm or higher. Interesting mid-IR sources have been developed using OPGaAs, including a narrow linewidth OPO operating between 10.3 and 10.9 µm [21], and a cascaded OPO tuning between 4 and 14 µm [22]. These both use nanosecond pulse pump lasers, as femtosecond lasers operating at a long enough wavelength are still a developing technology. A recent demonstration using a mode-locked Cr:ZnS laser operating at 2.35 µm has been used to generate a broad spectrum from 2.85 to 8.40 µm [23].

OPGaP has similar mid-IR transmission to ZGP (extending to 12 µm) but can be pumped at shorter wavelengths than ZGP or OPGaAs. OPGaP OPOs pumped by 1.5-µm

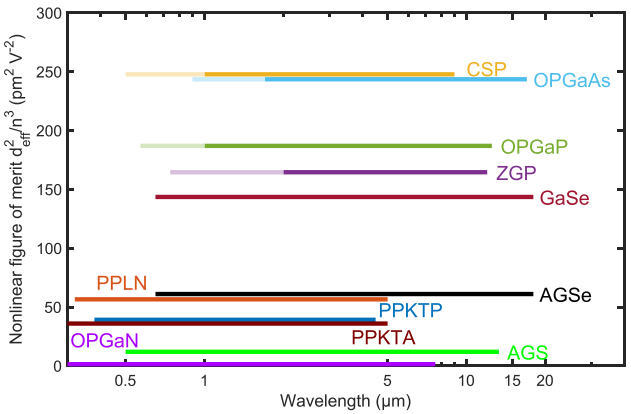

Fig. 1 Transmission range for commonly used nonlinear crystals with phasematching for mid-IR generation against their nonlinear figure of merit. This figure is adapted from [11] with additional information added on OPGaAs [12, 13], OPGaP [14, 15], ZGP [16], CSP [17, 18], PPLN [19] and PPKTP [20]. Greyed out regions show transmission which cannot be used for an OPO due to two-photon absorption or a lack of phasematching

pump lasers and generating mid-IR light have been demonstrated, including femtosecond frequency comb spanning 2.3–4.8 µm [24] and 3.5–5.0 µm [25]. Utilising the transparency of OPGaP, Lee et al. used an erbium fiber laser which was spectrally broadened and amplified with a thulium amplifier to mix 1.5 and 2 µm for difference frequency generation (DFG) producing tunable and spectrally broad 6–11 µm output with up to 70 mW of average power [26]. Recent work uses DFG of the different spectral components from a 1.5-µm erbium fiber laser broadened in nonlinear fiber to produce a frequency comb spanning 4–12 µm, and demonstrates dual-comb spectroscopy (DCS) over this broad spectrum [27].

As with CSP, mature 1-µm laser sources can also be used to pump OPGaP. DFG and optical parametric generation (OPG) have been demonstrated with nanosecond and picosecond pulse 1-µm lasers [28–30], but the mid-IR wavelengths generated were around 3 µm, which fails to take advantage of OPGaP's transparency range up to 12 µm. DFG between continuous-wave lasers was used to generate 3.40 µm [31] and 5.85 µm [32] in OPGaP. The first OPGaP optical parametric oscillator (OPO) pumped with a 1-µm laser-generated nanosecond mid-IR pulses at 4.6 µm [14]. We previously demonstrated the first 1-µm-pumped OPGaP OPO producing mid-IR beyond the transparency range of PPLN, using a modelocked fiber laser producing 200-fs pulses at 1040 nm, achieving tuning to 12-µm using a range of different OPGaP grating periods [33], and also demonstrated mid-IR DCS with dual OPGaP OPOs [34].

Some other nonlinear materials can be used to generate mid-IR light. Silver gallium selenide (AGSe) was used by Steinle et al. for DFG between a 1-µm pump laser and OPO to generate 4.5–20 µm with tens of mW of power [35]. A broad spectrum spanning 6.8–16.4 µm with 103 mW average power using DFG in lithium gallium sulphide (LGS) has been demonstrated [36], relying on the use of a very powerful 90 W thin-disc pump laser (LGS is not displayed on Fig. 1 as it has a very low nonlinear figure of merit, it was chosen in [36] for its thermal conductivity, high damage threshold and favourable phase matching). A newly developed material, barium gallium selenide, has been used with a nanosecond 1-µm pump laser to generate between 2.7 and 17 µm [37]. These materials, as well as others, can be used for DFG in the long-wave mid-IR, however, they are less versatile than OPGaAs and OPGaP due to the lack of suitable quasi-phasematching techniques, meaning that the maximum nonlinear coefficient cannot always be exploited. In general, the maximum nonlinear figure of merit is also lower than the semiconductor materials CSP, OPGaP, OPGaAs and ZGP (see Fig. 1). GaSe, the only material with a comparable figure of merit, has limited applications as the crystal is impossible to cut at certain phase-matching angles and it suffers from high linear absorption [36].

As this summary illustrates, practical choices for long-wave mid-IR generation with an optimal choice of pump laser and tuning range are very limited. In many applications, OPGaP can therefore be considered the material of choice, and in this article, we describe OPGaP OPOs using both femtosecond and picosecond 1-μm pump lasers, which produce mid-IR radiation at longer wavelengths than can be achieved with PPLN. We present the mid-IR spectra produced by the OPOs, and introduce an investigation of temperature tuning to extend the wavelength coverage to even long wavelengths than are available from room temperature operation.

2 Femtosecond OPGaP OPO

We report here the further optimisation of our previously reported OPGaP OPO [33]. The OPO layout is shown in Fig. 2a. The OPO is synchronously pumped by a passively modelocked all normal dispersion Yb:fiber laser producing 101.2-MHz chirped output pulse with approximately 800-fs duration and a centre wavelength of 1037 nm. These pulses are amplified in a cladding-pumped Yb fiber amplifier, pumped using a 10-W, 976- nm multimode diode laser. The pulses are compressed in a transmission grating pulse compressor to a minimum duration of around 150 fs (a little longer than the Fourier transform limit due to third-order dispersion in the amplifier). After an optical isolator and the pulse compressor there is 2.2 W average power for pumping the OPO. The OPO cavity is a simple ring cavity with the crystal in the centre of two spherical mirrors of 100-mm radius of curvature. The beam is expanded to a waist of 2 mm to allow it to be focused to an approximately 17-μm waist in the middle of the OPGaP crystal (this is to match the signal mode of ~ 19 μm from cavity stability calculations, though it varies slightly for different signal wavelengths). The first curved cavity mirror and the two plane mirrors are on zinc selenide (ZnSe) substrates, coated for high transmission of the pump (1.02–1.06 μm) and idler (7–13 μm). The second curved mirror is a silver mirror which reflected all three beams. The OPGaP crystals used had a useable aperture of around 200 μm, determined by the propagation of the grating structure during fabrication. Figure 2b shows the typical grating propagation achieved in the OPGaP growth process.

The OPO was aligned using the second harmonic green light generated in the OPGaP. The cavity length was matched to the repetition rate of the laser. Each OPGaP crystal used

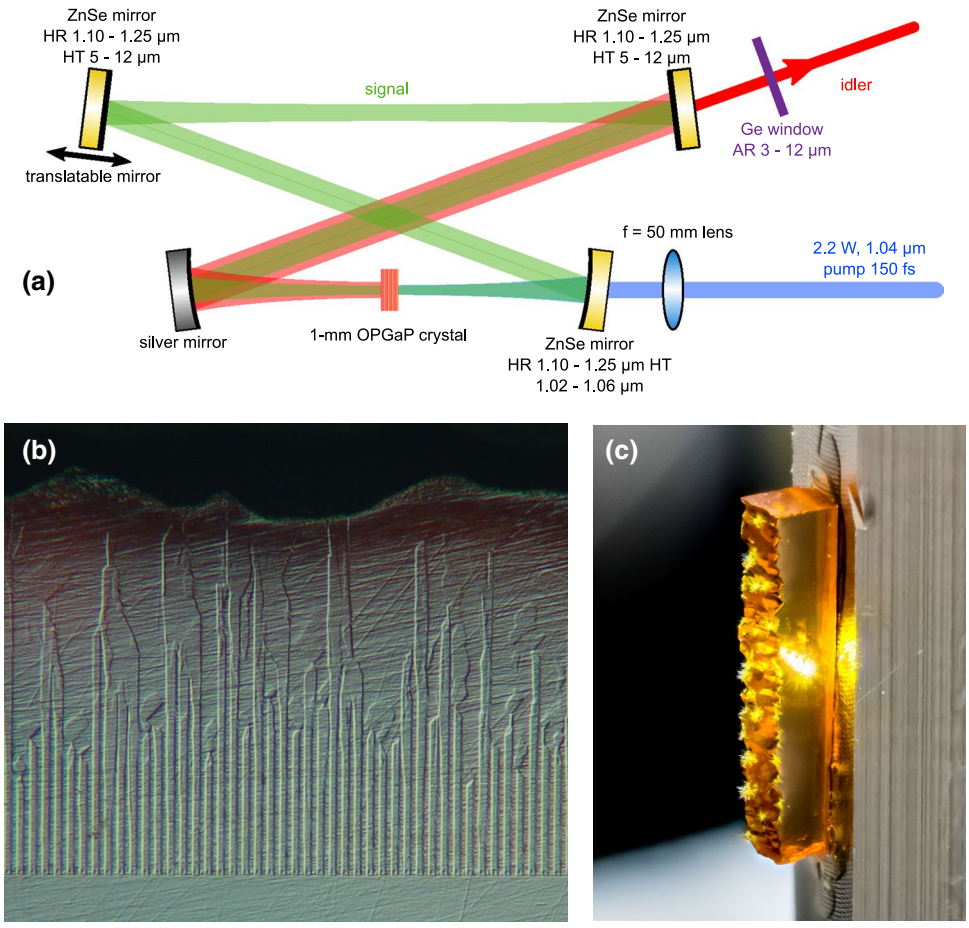

Fig. 2 **a** Femtosecond OPGaP OPO layout. **b** Microscopic cross-sectional image of 31-μm grating period. **c** Photograph of 21.5-μm grating period inside oscillating OPO cavity. The visible yellow light is unphasematched sum frequency generation between the signal and pump wavelengths

had a single grating period and was 1 mm in length. Using a range of seven different gratings from 21.5 to 34.0 µm, the centre wavelength of the idler output could be tuned from 5.5 to 11.8 µm when the crystal was operated at room temperature. The idler beam from the OPO was transmitted through the first plane cavity mirror, and the undepleted pump was removed using a germanium window. We observed higher average idler power than in our previous report [33], with up to 105 mW recorded at 5.5 µm. This improvement is partly due to optimisation of the pump focusing. We also found that a slight increase in the pump pulse duration (by reducing the separation of the gratings in the pulse compressor) improved the output power. There is no dispersion compensation in the OPO cavity, so it is likely that adding some group delay dispersion to the pump pulses helps it more closely match the cavity dispersion and improves efficiency, although we have not characterised this. The idler spectrum for each grating was measured using a Fourier transform spectrometer containing a liquid nitrogen-cooled HgCdTe detector sensitive from 3 to 12 µm. The measured spectra and the corresponding average power are shown in Fig. 3.

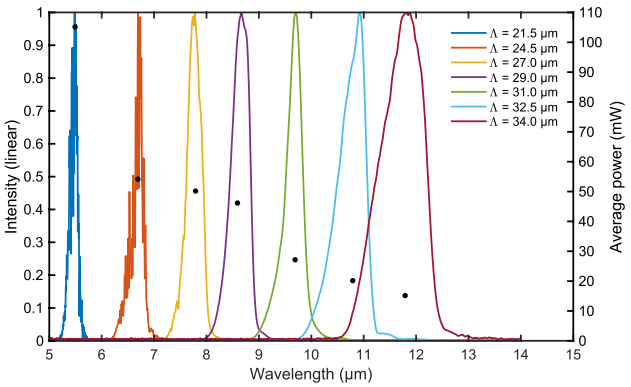

Fig. 3 Idler spectra measured at 1.2-cm^{-1} resolution, and average output power for seven different OPGaP grating periods

Without any electronic stabilisation, the OPO was passively stable enough for several minutes without significant change in the output power or spectrum, but drifted over longer time intervals. The spectra in Fig. 3 are measured at the maximum idler power, and only a slight degree of cavity length tuning was observed.

Until very recently, the Sellmeier equation measured by Parsons and Coleman [38] was the standard equation to use. Despite being measured at far-infrared wavelengths, it was observed to predict the refractive index of gallium phosphide very well in the near- and mid-infrared. It is only valid at room temperature, and the only temperature-dependent Sellmeier that had been measured until very recently did not extend past 5.5-µm wavelength. Very recently, Wei et al. reported a Sellmeier equation which covered 0.7–12.5 µm over a wide temperature range 78–450 K [39].

We tested the predictions of this equation with an OPO very similar to that shown in Fig. 2a, using a simple temperature control system for the OPGaP crystal consisting of a power resistor for heating and a thermistor to monitor. Using a small 1.0 × 1.0 × 1.1-mm OPGaP crystal with a 31-µm grating period, the maximum temperature the crystal could reach was 400 K. In Fig. 4a, the idler spectrum from the OPO is presented, and compared with the spectrum measured at 293 K from the previous OPO configuration. Also shown are the peak wavelengths expected from a phase-matching calculation using the new temperature-dependent Sellmeier equation. The spectrum measured at 400 K is slightly longer in wavelength than predicted by the calculation.

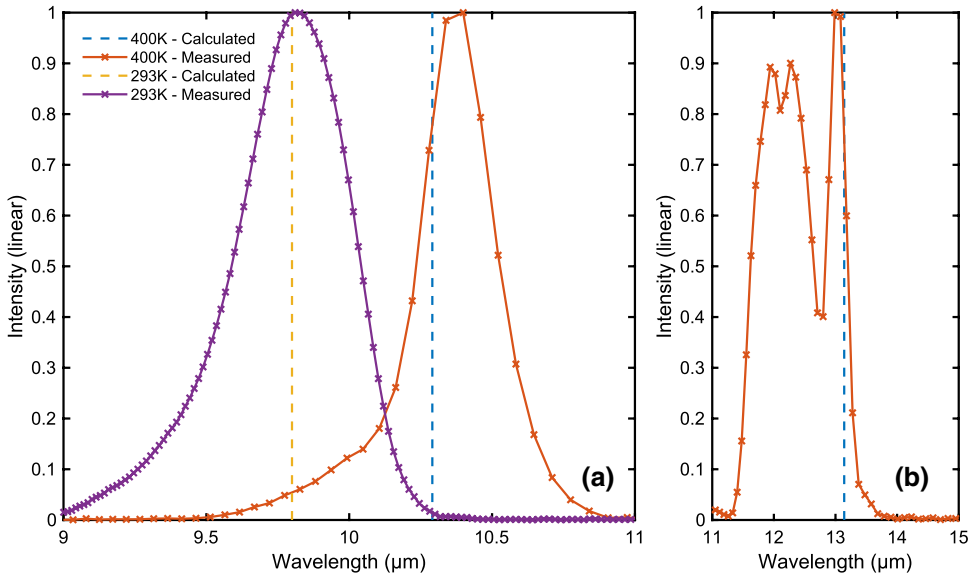

Fig. 4 **a** Spectra from OPO with 31-µm OPGaP grating at 400K (orange, measured with 6-cm^{-1} resolution) and 293K (purple, measured with 2-cm^{-1} resolution). The dotted lines show the calculated peak wavelength from the Sellmeier equation in [39]. **b** Spectrum from OPO with 34-µm OPGaP grating at 400K (orange, measured with 6-cm^{-1} resolution)

We also measured the spectrum of an OPO using the 34-μm OPGaP grating at 400 K, which is shown in Fig. 4b. The spectrum shifts longer in wavelength to cover beyond 13 μm. At this wavelength, the spectral measurement is influenced by a severe roll off in the sensitivity of the HgCdTe detector after 12 μm. To further illustrate the temperature-tuning possibilities, Fig. 5 presents the calculated temperature tuning. Signal and idler centre wavelengths are presented as a function of temperature for a range of grating periods.

3 Picosecond OPGaP OPO

Difference-frequency mixing using OPGaP with both nanosecond and picosecond pump pulses at 1-μm wavelength has been explored [28, 29], as well as with a continuous-wave pump [32] (as discussed in the introduction). At a wavelength of 1064 nm, the linear absorption of gallium phosphide should be low, though significant linear absorption was observed by Casals et al. in their OPGaP experiments [29]. They reported only 52% transmission at 1064 nm through a 40-mm OPGaP crystal with a 16-μm grating period. This absorption could be due to impurities inadvertently added to the gallium phosphide during the fabrication process.

In this section, we report a 1064-nm synchronously pumped picosecond OPO. The pump laser used was an 80-MHz modelocked laser with 8.5-ps pulses at 1064 nm (0.7-nm FWHM) producing an average output power of up to 5 W. The OPGaP crystals used were 23.9 mm in length with a grating period of 29 μm. We observed 70% transmission at the pump wavelength (yielding an absorption coefficient of 0.15 cm^{-1}), consistent with the absorption loss observed by Casals et al. [29]. A ring cavity with 200-mm radius-of-curvature mirrors was configured to match the repetition rate of the pump laser. The signal beam waist of the cavity from resonator stability calculations was 53 μm, and the pump beam was focused through a curved cavity mirror to around 50 μm in the centre of the OPGaP crystal to closely mode match the signal. The first cavity mirror was a ZnSe substrate coated for high transmission from 1.02 to 1.06 μm, and high reflection for 1.15–1.35 μm. The second-curved mirror was silver coated, to reflect the pump, signal and idler beams. The first plane-folding mirror was a ZnSe mirror coated for high reflection for 1.15–1.35 μm and high transmission for pump (1.02–1.06 μm) and idler (5–12 μm) wavelengths. The collimated idler beam and undepleted pump exited the cavity here, and the undepleted pump was separated from the idler using a germanium window. The second plane cavity mirror was a gold cavity mirror, which we used rather than another dielectric mirror as it made the OPO alignment easier. The OPO layout is shown in Fig. 6a.

Pumped at 1064 nm, the 29-μm OPGaP grating at room temperature was calculated to phase match for a signal of 1.23 μm and idler of 7.87 μm using the Sellmeier equation from Parsons and Coleman [38] (which is identical to the equation from [39] at room temperature). The walk-off between signal and pump in 23.9 mm was 6 ps, ensuring good overlap through the length of the crystal. By aligning the cavity using the pump light, and matching the cavity length precisely to the 80-MHz repetition rate using a mirror mounted on a micrometer-adjusted translation stage, we achieved oscillation of the signal. With no signal output coupler, we used the idler power to optimise the alignment of the OPO cavity. The output power of the cavity was then measured as a function of the input pump power, and is shown in Fig. 6b. After losses in an optical isolator and beam steering optics, the available pump power was 3.6 W. A maximum idler output power of 137 mW was observed. As the pump power was increased, the idler power did not increase linearly—the efficiency began decreasing after about 2 W pump power. This could be due to the lack of

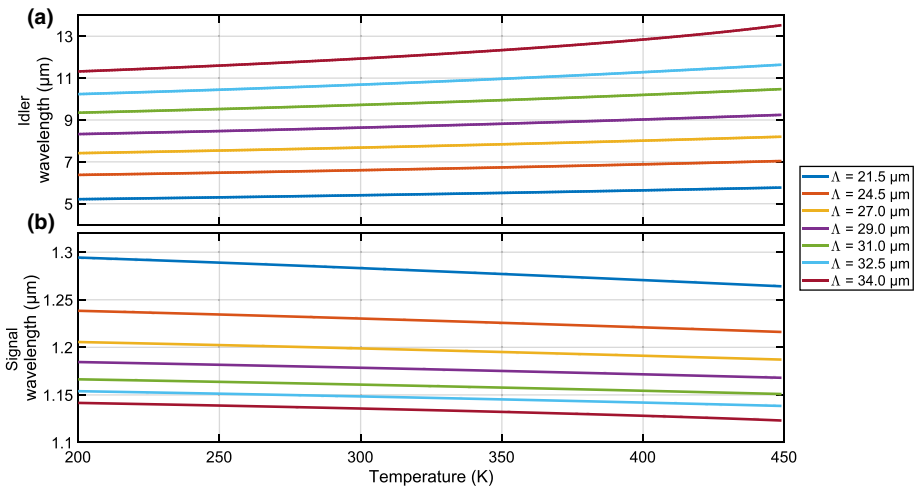

Fig. 5 Calculated centre idler (**a**) and signal (**b**) wavelengths as a function of temperature with a pump wavelength of 1037 nm, for a range of grating periods

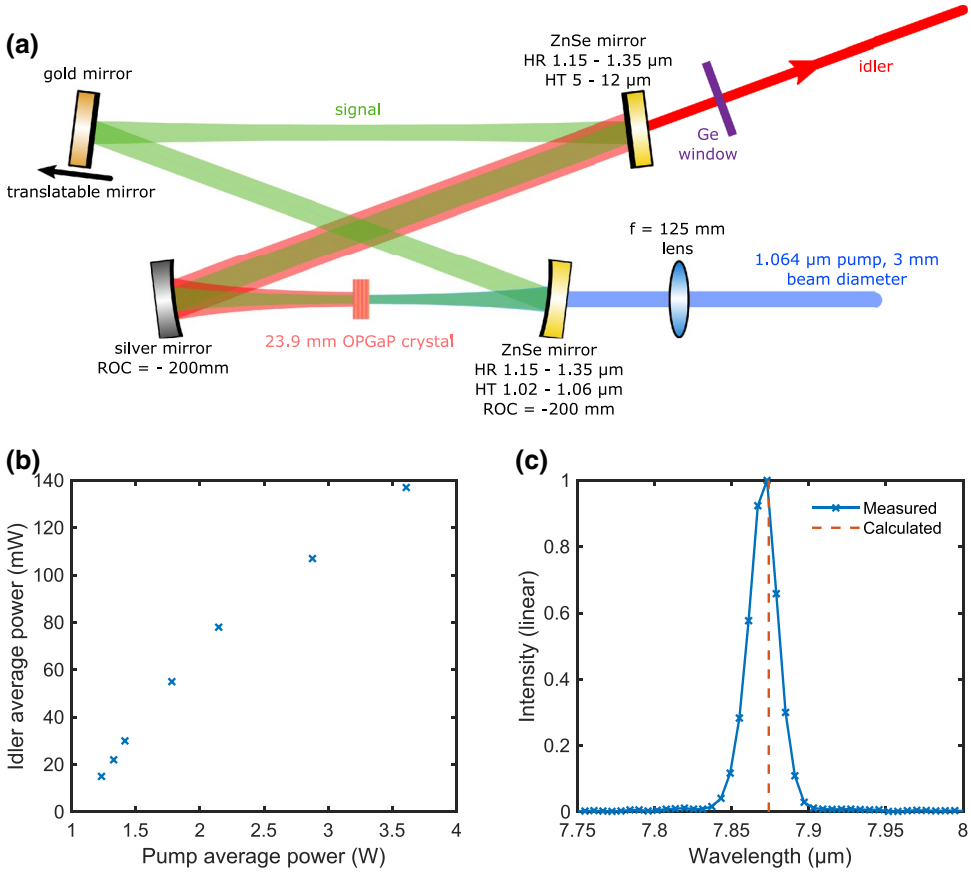

Fig. 6 **a** Picosecond OPO layout. **b** Output idler power recorded as a function of wavelength. **c** Idler spectrum measured at 1.0 cm^{-1} (blue) and centre idler wavelength calculated using Sellmeier equation from [38]

signal output coupling causing more back conversion as the pump power was increased.

The idler wavelength was calculated to be 7.87 μm, and we also directly measured the idler wavelength with a home-made Fourier transform spectrometer (configured with CaF_2 beam splitter for 2–8 μm and thermo-electrically cooled MCT detector). The measured spectrum is shown in Fig. 6c with the calculated peak idler wavelength also illustrated. The measurement agrees with the calculation within the resolution error. The maximum idler power was measured at a particular cavity length, but the cavity length could be tuned over 370 μm while still maintaining oscillation. No change in the wavelength of the idler beam was observed over the tuning range. The pulse duration of the idler output was not measured. The FWHM of the idler spectrum of 21 nm means the time bandwidth product would be 0.86 if the pulse duration matched the 8.5 ps of the pump pulses, and could be compressed to 3.1 ps ($sech^2(t)$ pulse shape).

4 Discussion and conclusions

It was noted by Morz et al. that OPOs require significant stabilisation for sensitive applications [2], and this is certainly true for application such as microspectroscopy and DCS (as we have demonstrated separately [34]). The passive stability of our fs OPO described here is still suitable for many applications. An example is our work on the mid-IR spectroscopy of aerosols [40], where measurements of scattered light by aerosol particles were made across a wavelength range 7–11 μm, which would have been impossible with an incoherent source and more challenging with a narrow linewidth tunable laser.

The recently demonstrated dual-comb spectroscopy by Timmers et al. [27] is a clear demonstration of the advantages of OPGaP over alternative nonlinear materials as well as QCLs. The high-resolution measurements at millisecond acquisition times of a wide mid-IR spectrum from 4 to 12 μm covering much of the molecular fingerprint region represent a huge milestone in the development of mid-infrared coherent sources. OPGaP OPO combs will not be able to cover such a broad spectrum at once, but may still have an advantage in average power, as the DFG comb of [27] generated hundreds of μW, while we have shown in this article that OPOs can readily reach 100 mW.

As well as DCS, another recent development in mid-IR spectroscopy is field-resolved spectroscopy (FRS). FRS uses an ultrafast mid-IR pulse to excite molecular absorption modes and then measures the electric field of the decay of the excited modes using electro-optic sampling. Where

DCS facilitates very high-resolution spectral measurements, FRS promises unparalleled sensitivity and dynamic range in mid-IR absorption measurements. The first proposals of FRS [41, 42] have used a DFG source based on GaSe which uses a high-power 90-W thin-disc pump laser [36]. As reported in [27], OPGaP can be used to produce very short mid-IR pulses with only 350 mW of pump power. OPGaP is therefore a very promising material for future mid-IR spectroscopy embodiments, which could include FRS or other uses of the short pulse duration possible (such as pump–probe spectroscopy).

In conclusion, here we have presented improved performance from a synchronously pumped femtosecond OPGaP OPO and introduced a synchronously pumped picosecond OPGaP OPO, both pumped by routinely available 1-μm lasers and generating coherent mid-IR at wavelengths beyond the transparency range of PPLN and other commonly used nonlinear materials.

References

1. F. Zhu, J. Xia, A. Bicer, J. Bounds, A. Kolomenskii, J. Strohaber, L. Johnson, M. Amani, H. Schuessler, Appl. Opt. **56**, 6311 (2017)
2. F. Mörz, R. Semenyshyn, T. Steinle, F. Neubrech, U. Zschieschang, H. Klauk, A. Steinmann, H. Giessen, Opt. Express **25**, 32355 (2017)
3. Y. Yao, A.J. Hoffman, C.F. Gmachl, Nat. Photon. **6**, 432 (2012)
4. R. Ostendorf, L. Butschek, S. Hugger, F. Fuchs, Q. Yang, J. Jarvis, C. Schilling, M. Rattunde, A. Merten, J. Grahmann, D. Boskovic, T. Tybussek, K. Rieblinger, J. Wagner, Photonics **3**, 28 (2016)
5. D.R.S.D. Solutions, MIRcat-QT™ Mid-IR Laser, https://www.daylightsolutions.com/product/mircat/. Accessed 17 June 2018
6. I. Coddington, N. Newbury, W. Swann, Optica **3**, 414 (2016)
7. R.W. Boyd, *Nonlinear Optics*, 3rd edn. (Academic Press, Cambridge, 2008)
8. S. Chaitanya Kumar, P.G. Schunemann, K.T. Zawilski, M. Ebrahim-Zadeh, J. Opt. Soc. Am. B **33**, D44 (2016)
9. H. Liang, P. Krogen, Z. Wang, H. Park, T. Kroh, K. Zawilski, P. Schunemann, J. Moses, L.F. Dimauro, F.X. Kärtner, K. Hong, Nat. Commun. **8**, 141 (2017)
10. D. Sanchez, M. Hemmer, M. Baudisch, S.L. Cousin, K. Zawilski, P. Schunemann, O. Chalus, C. Simon-Boisson, J. Biegert, Optica **3**, 147 (2016)
11. P.G. Schunemann, K.T. Zawilski, L.A. Pomeranz, D.J. Creeden, P.A. Budnui, J. Opt. Soc. Am. B **33**, 36 (2016)
12. K.L. Vodopyanov, O. Levi, P.S. Kuo, T.J. Pinguet, J.S. Harris, M.M. Fejer, B. Gerard, L. Becouarn, E. Lallier, Opt. Lett. **29**, 1912 (2004)
13. W.C. Hurlbut, K.L. Vodopyanov, P.S. Kuo, M.M. Fejer, Y.S. Lee, Opt. Lett. **32**, 668 (2007)
14. L.A. Pomeranz, P.G. Schunemann, D.J. Magarrell, J.C. McCarthy, K.T. Zawilski, D.E. Zelmon, Proc. SPIE **9347**, 93470K, (2015)
15. J. Václavík, D. Vápenka, EPJ Web Conf. **48**, 28 (2013)
16. M. Henriksson, M. Tiihonen, V. Pasiskevicius, F. Laurell, Appl. Phys. B Lasers Opt. **88**, 37 (2007)
17. Z. Zhang, D.T. Reid, S. Chaitanya Kumar, M. Ebrahim-Zadeh, P.G. Schunemann, K.T. Zawilski, C.R. Howle, Opt. Lett. **38**, 5110 (2013)
18. F.K. Hopkins, S. Guha, B. Claflin, P.G. Schunemann, K.T. Zawilski, N.C. Giles, L.E. Halliburton, Proc SPIE **9616**, 96160W (2015)
19. Covesion, MgO:PPLN crystals. https://www.covesion.com/products/magnesium-doped-ppln-mgoppln-crystals/. Accessed 17 June 2018
20. G. Hansson, H. Karlsson, S. Wang, F. Laurell, Appl. Opt. **39**, 5058 (2000)
21. Q. Clément, J. Melkonian, J. Dherbecourt, M. Raybaut, A. Grisard, E. Lallier, B. Gerard, B. Faure, G. Souhaité, A. Godard, Opt. Lett. **40**, 2676 (2015)
22. K.L. Vodopyanov, I. Makasyuk, P.G. Schunemann, Opt. Express **22**, 4131 (2014)
23. Q. Ru, K. Zhong, N.P. Lee, Z.E. Loparo, P.G. Schunemann, S. Vasilyev, S.B. Mirov, K.L. Vodopyanov, Instantaneous spectral span of 2.85–8.40 μm achieved in a Cr:ZnS laser pumped subharmonic GaAs OPO, in *Conference on Lasers and Electro-Optics*. OSA Technical Digest (online) (Optical Society of America, 2017), paper SM4M.3
24. Q. Ru, Z.E. Loparo, X. Zhang, S. Crystal, S. Vasu, P.G. Schunemann, K.L. Vodopyanov, Opt. Lett. **42**, 4756 (2017)
25. E. Sorokin, A. Marandi, P.G. Schunemann, M. Fejer, I.T. Sorokina, R.L. Byer, Three-optical-cycle frequency comb centered around 4.2 μm using OP-GaP-based half-harmonic generation, in *High-Brightness Sources and Light-Driven Interactions*. OSA Technical Digest (online) (Optical Society of America, 2016), paper MS3C.2
26. K.F. Lee, C.J. Hensley, P.G. Schunemann, M.E. Fermann, Opt. Express **25**, 17411 (2017)
27. H. Timmers, A. Kowligy, A. Lind, F.C. Cruz, N. Nader, M. Silfies, T.K. Allison, G. Ycas, P.G. Schunemann, S.B. Papp, S.A. Diddams, Optica **5**, 727–732 (2018)
28. J. Wei, S.C. Kumar, H. Ye, K. Devi, P.G. Schunemann, M. Ebrahim-Zadeh, Opt. Lett. **42**, 2193 (2017)
29. J.C. Casals, S. Parsa, S.C. Kumar, K. Devi, P.G. Schunemann, M. Ebrahim-Zadeh, Opt. Express **25**, 19595 (2017)
30. H. Ye, S. Chaitanya Kumar, J. Wei, P.G. Schunemann, M. Ebrahim-Zadeh, Opt. Lett. **42**, 3694 (2017)
31. S. Guha, J.O. Barnes, P.G. Schunemann, Opt. Mater. Express **5**, 2911 (2015)
32. G. Insero, C. Clivati, D. D'Ambrosio, P. De Natale, G. Santambrogio, P.G. Schunemann, J.J. Zondy, S. Borri, Opt. Lett. **41**, 5114 (2017)
33. L. Maidment, P.G. Schunemann, D.T. Reid, Opt. Lett. **41**, 4261 (2016)
34. O. Kara, L. Maidment, T. Gardiner, P.G. Schunemann, D.T. Reid, Opt. Express **25**, 32713 (2017)
35. T. Steinle, F. Mörz, A. Steinmann, H. Giessen, Opt. Lett. **41**, 4863 (2016)
36. I. Pupeza, D. Sánchez, J. Zhang, N. Lilienfein, M. Seidel, N. Karpowicz, I. Znakovskaya, M. Pescher, W. Schweinberger, V. Pervak, E. Fill, O. Pronin, Z. Wei, F. Krausz, A. Apolonski, J. Biegert, Nat. Photon. **9**, 721 (2015)
37. N.Y. Kostyukova, A.A. Boyko, V. Badikov, D. Badikov, G. Shevyrdyaeva, V. Panyutin, G.M. Marchev, D.B. Kolker, V. Petrov, Opt. Lett. **41**, 3667 (2016)
38. D.F. Parsons, P.D. Coleman, Appl. Opt. **10**, 1683 (1971)

39. J. Wei, J.M. Murray, J.O. Barnes, D.M. Krein, P.G. Schunemann, S. Guha, Opt. Mater. Express **8**, 485 (2018)
40. L. Maidment, R.J. Clewes, M.D. Bowditch, C.R. Howle, D.T. Reid, Infrared fingerprint-region aerosol spectroscopy, in *Conference on Lasers and Electro-Optics*. OSA Technical Digest (online) (Optical Society of America, 2017), paper SF1M.3
41. I. Pupeza, M. Huber, W. Schweinberger, M. Trubetskov, S.A. Hussain, L. Vamos, O. Pronin, F. Habel, V. Pervak, N. Karpowicz, E. Fill, A. Apolonski, M. Zigman, A.M. Azzeer, F. Krausz, Field-resolved spectroscopy in the molecular fingerprint region, in *2017 European Conference on Lasers and Electro-Optics and European Quantum Electronics Conference*. (Optical Society of America, 2017), paper CH_2_4
42. A. Apolonskiy, I. Pupeza, F. Krausz, E. Fill, Patent application: US20180003623A1